Chiral-odd generalized parton distributions for proton in a light-front quark-diquark model

Dipankar Chakrabarti and Chandan Mondal

Department of Physics, Indian Institute of Technology Kanpur, Kanpur 208016, India
(Received 3 September 2015; published 8 October 2015)

We present a study of the chiral-odd generalized parton distributions (GPDs) for u and d quarks in a proton using the light-front wave functions (LFWFs) of the scalar quark-diquark model for a nucleon constructed from the soft-wall AdS/QCD correspondence. We obtain the GPDs in terms of overlaps of the LFWFs. Numerical results for chiral-odd GPDs in momentum as well as transverse position (impact) spaces considering both zero and nonzero skewness(ζ) are presented. For nonzero skewness, the GPDs are also evaluated in longitudinal position space.

I. INTRODUCTION

Generalized parton distributions (GPDs) encode information about the three-dimensional spatial structure of the proton as well as the spin and orbital angular momentum of the constituents. The GPDs (see Ref. [1] for reviews on GPDs) are off-forward matrix elements and appear in the exclusive processes like deeply virtual Compton scattering (DVCS) or vector-meson productions. The GPDs being functions of three variables (namely, the longitudinal momentum fraction x of the parton, the square of the total momentum transferred t, and the longitudinal momentum transferred or the so-called skewness ζ in the process) contain more information than the ordinary parton distribution functions (PDFs). The first moments of GPDs give the form factors accessible in exclusive processes, whereas they reduce to PDFs in the forward limit. At leading twist, we can define three generalized distributions in parallel to three PDFs, namely, the unpolarized, helicity, and transversity distributions. Similar to the transversity distribution, the generalized transversity distribution F_T is also chiral-odd. In the most general way, F_T is parametrized in terms of four chiral-odd GPDs, namely H_T, $\tilde{H}_T$, E_T, and $\tilde{E}_T$ [2–5]. The chiral-odd GPDs give information on the correlation between the spin and angular momentum of quarks inside the proton. At zero skewness, by performing a Fourier transform (FT) of the GPDs with respect to the momentum transfer in the transverse direction $\Delta_\perp$, one obtains the impact-parameter-dependent parton distributions, which provide us with the picture of how the partons of a given longitudinal momentum fraction (x) are distributed in impact parameter ($b_\perp$) or transverse position space. Unlike the GPDs themselves, impact-parameter-dependent parton distributions have a probabilistic interpretation and satisfy the positivity condition [5–7]. In the $t \to 0$ limit, the second moment of the GPDs are related to the angular momentum contribution to the nucleon by the quark or gluon [8]. The impact-parameter-dependent PDFs are transversely distorted when one considers transversely

polarized nucleons. The transverse distortion can also be connected with Ji's angular momentum relation. An interesting interpretation of Ji's angular momentum sum rule [8] for a transversely polarized state was obtained in terms of the impact-paramete-ependent PDFs in Ref. [5]. For the unpolarized quark, transverse distortion arises due to the chiral-even GPD E which is related to the anomalous magnetic moment of the quarks. As far as the transverse distortion of transversely polarized quark distributions is concerned, the linear combination of chiral-odd GPDs $(2\tilde{H}_T + E_T)$ plays a role similar to the GPD E in the unpolarized quark distributions. In the forward limit, a relation between the transverse total angular momentum of the quarks and a combination of the second moments of H_T, $\tilde{H}_T$, and E_T has been proposed in Ref. [5], in analogy with Ji's relation. $\tilde{E}_T$, being an odd function of ζ, does not contribute at $\zeta = 0$. For nonzero skewness one can also represent the GPDs in the longitudinal position space by taking the FT of the GPDs with respect to ζ [9–14].

Unlike the chiral-even GPDs, it is very difficult to measure chiral-odd GPDs. In a very recent COMPASS experiment [15], the exclusive production of ρ^0 mesons by scattering muons off transversely polarized protons was measured. The target spin asymmetries measured in the experiment agree well with GPD-based model calculations which indicate the first experimental evidence of chiral-odd GPDs, especially the transversity GPD H_T. There have been proposals to get access to the chiral-odd GPDs through diffractive double meson production [16,17]. The role of transversity GPDs in the leptoproduction of vector mesons [18] as well as in hard exclusive electroproduction of pseudoscalar mesons [19] has been investigated within the framework of the handbag approach. A simple model for the dominant transversity GPD H_T based on the concept of double distribution has been proposed and has been used to estimate the unpolarized differential cross section for this process in the kinematics of the JLab and COMPASS experiments in Ref. [20]. The chiral-odd GPDs in a constituent quark model have been

studied for nonzero skewness using the overlap representation in terms of light-front wave functions (LFWFs) in Ref. [3]. The general properties of the chiral-odd GPDs in a QED model have been investigated in momentum space, transverse position, and longitudinal position spaces [9]; the impact parameter representation of the GPDs have been studied in a QED model of a dressed electron [10] and in a quark-diquark model [21] for $\zeta = 0$. The Mellin moments of the transverse GPDs have been evaluated on the lattice [22–25].

There have been numerous attempts to gain insight into the hadron structure by studying QCD-inspired models as nonperturbative properties of hadrons are always very difficult to evaluate from QCD first principles. In this work, we consider a phenomenological light-front quark-diquark model recently proposed by Gutsche *et al.* [26] where the LFWFs are modeled by the wave functions obtained from a soft-wall model in the light-front AdS/QCD correspondence [27,28]. This model is consistent with the Drell-Yan-West relation which relates the high-Q^2 behavior of the nucleon form factors and the large-x

behavior of the structure functions. The chiral-even GPDs for zero skewness with arbitrary twist have been discussed in Ref. [26]. The chiral-even GPDs have been studied in both hard-wall and soft-wall models in AdS/QCD [29,30] and in the light-front quark-diquark model for both zero and nonzero skewness [14].

The paper is organized in the following way. In Sec. II, a brief introduction about the nucleon LFWFs of the quark-diquark model is given. We present the overlap formalism of the chiral-odd GPDs and show the results for proton GPDs of u and d quarks in momentum space in Sec. III. The GPDs in the transverse as well as the longitudinal impact parameter space are presented in Secs. IV and IV A. Finally, we summarize all the results in Sec. V.

II. LIGHT-FRONT QUARK-DIQUARK MODEL FOR THE NUCLEON

Here, we consider the quark-diquark model with a scalar diquark. The two-particle Fock-state expansions for $J^z = +\frac{1}{2}$ and $J^z = -\frac{1}{2}$ are then written as

$$|P; +\rangle = \sum_q \int \frac{dx\, d^2\mathbf{k}_\perp}{2(2\pi)^3 \sqrt{x(1-x)}} \left[\psi^+_{+q}(x, \mathbf{k}_\perp) \left| +\frac{1}{2}, 0; xP^+, \mathbf{k}_\perp \right\rangle + \psi^+_{-q}(x, \mathbf{k}_\perp) \left| -\frac{1}{2}, 0; xP^+, \mathbf{k}_\perp \right\rangle \right], \quad (1)$$

$$|P; -\rangle = \sum_q \int \frac{dx\, d^2\mathbf{k}_\perp}{2(2\pi)^3 \sqrt{x(1-x)}} \left[\psi^-_{+q}(x, \mathbf{k}_\perp) \left| +\frac{1}{2}, 0; xP^+, \mathbf{k}_\perp \right\rangle + \psi^-_{-q}(x, \mathbf{k}_\perp) \left| -\frac{1}{2}, 0; xP^+, \mathbf{k}_\perp \right\rangle \right], \quad (2)$$

where $|\lambda_q, \lambda_s; xP^+, \mathbf{k}_\perp\rangle$ represents a two-particle state with a quark spin $\lambda_q = \pm$, longitudinal momentum xP^+, and a spectator of spin $\lambda_s = 0$ (scalar diquark). The states are normalized as

$$\langle \lambda'_q, \lambda'_s; x'P^+, \mathbf{k}'_\perp | \lambda_q \lambda_s; xP^+, \mathbf{k}_\perp \rangle$$
$$= \prod_{i=1}^{2} 16\pi^3 p_i^+ \delta(p'^+_i - p_i^+) \delta^2(\mathbf{k}'_{\perp i} - \mathbf{k}_{\perp i}) \delta_{\lambda'_i \lambda_i}, \quad (3)$$

and $\psi^{\lambda_N}_{\lambda_q q}$ are the light-front wave functions with nucleon helicities $\lambda_N = \pm$ and quark helicities $\lambda_q = \pm$. We adopt the generic ansatz for the quark-diquark model of the valence Fock state of the nucleon LFWFs at an initial scale $\mu_0 = 313$ MeV as proposed in Ref. [26]:

$$\psi^+_{+q}(x, \mathbf{k}_\perp) = \varphi^{(1)}_q(x, \mathbf{k}_\perp),$$
$$\psi^+_{-q}(x, \mathbf{k}_\perp) = -\frac{k^1 + ik^2}{xM} \varphi^{(2)}_q(x, \mathbf{k}_\perp),$$
$$\psi^-_{+q}(x, \mathbf{k}_\perp) = \frac{k^1 - ik^2}{xM} \varphi^{(2)}_q(x, \mathbf{k}_\perp),$$
$$\psi^-_{-q}(x, \mathbf{k}_\perp) = \varphi^{(1)}_q(x, \mathbf{k}_\perp), \quad (4)$$

where

$$\varphi^{(i)}_q(x, \mathbf{k}_\perp) = N^{(i)}_q \frac{4\pi}{\kappa} \sqrt{\frac{\log(1/x)}{1-x}} x^{a^{(i)}_q} (1-x)^{b^{(i)}_q}$$
$$\times \exp\left[-\frac{\mathbf{k}^2_\perp}{2\kappa^2} \frac{\log(1/x)}{(1-x)^2} \right] \quad (5)$$

is the modified version of the AdS/QCD prediction for the two-particle wave function. For $a^{(i)}_q = b^{(i)}_q = 0$, $\varphi^{(i)}_q(x, \mathbf{k}_\perp)$ reduces to the AdS/QCD prediction [28]. κ is the AdS/QCD scale parameter which is taken to be 0.4 GeV [30,31]. The parameters $a^{(i)}_q$ and $b^{(i)}_q$ with the constants $N^{(i)}_q$ are fixed by fitting the electromagnetic properties of the nucleons: $a^{(1)}_u = 0.020$, $a^{(1)}_d = 0.10$, $b^{(1)}_u = 0.022$, $b^{(1)}_d = 0.38$, $a^{(2)}_u = 1.05$, $a^{(2)}_d = 1.07$, $b^{(2)}_u = -0.15$, $b^{(2)}_d = -0.20$, $N^{(1)}_u = 2.055$, $N^{(1)}_d = 1.7618$, $N^{(2)}_u = 1.322$, $N^{(2)}_d = -2.4827$. Although the parameters presented in Ref. [14] reproduce the nucleon electromagnetic properties, the normalizations of the wave functions were not correct. The results presented in Refs. [14,32] have numerically insignificant differrences when re-evaluated with the new parameters. Recently, a modified version of the diquark model was proposed in Ref. [33].

III. CHIRAL-ODD GENERALIZED PARTON DISTRIBUTIONS

The chiral-odd GPDs are defined as off-forward matrix elements of the bilocal operator of light-front correlation functions of the tensor current [2],

$$\frac{1}{2}\int\frac{dz^-}{2\pi}e^{i\bar{x}P^+z^-}\langle p',\lambda'|\bar{\psi}(-z/2)\sigma^{+i}\gamma_5\psi(z/2)|p,\lambda\rangle_{|_{z^+=0,\vec{z}_\perp=0}}$$

$$=\frac{1}{2P^+}\bar{u}(p',\lambda')\left[H_T^q\sigma^{+i}\gamma_5+\tilde{H}_T^q\frac{\epsilon^{+i\alpha\beta}\Delta_\alpha P_\beta}{M^2}\right.$$

$$\left.+E_T^q\frac{\epsilon^{+i\alpha\beta}\Delta_\alpha\gamma_\beta}{2M}+\tilde{E}_T^q\frac{\epsilon^{+i\alpha\beta}P_\alpha\gamma_\beta}{M}\right]u(p,\lambda),\qquad(6)$$

where $i=1,2$ is a transverse index. p (p') and $\lambda(\lambda')$ denote the proton momenta and the helicity of the initial (final) state of the proton, respectively. In the symmetric frame, the kinematical variables are

$$P^\mu=\frac{(p+p')^\mu}{2},\qquad\Delta^\mu=p'^\mu-p^\mu,\qquad\zeta=-\Delta^+/2P^+,$$
$$(7)$$

and $t=\Delta^2$. We choose the light-front gauge $A^+=0$, so that the gauge link appearing in between the quark fields in Eq. (6) is unity. The GPDs which involve the quark helicity flip can be related to the following matrix elements [2,3]:

$$A_{\lambda'+,\lambda-}=\int\frac{dz^-}{2\pi}e^{i\bar{x}P^+z^-}\langle p',\lambda'|\mathcal{O}_{+,-}(z)|p,\lambda\rangle|_{z^+=0,\vec{z}_\perp=0},$$

$$A_{\lambda'-,\lambda+}=\int\frac{dz^-}{2\pi}e^{i\bar{x}P^+z^-}\langle p',\lambda'|\mathcal{O}_{-,+}(z)|p,\lambda\rangle|_{z^+=0,\vec{z}_\perp=0},$$
$$(8)$$

with the operators $O_{+,-}$ and $O_{-,+}$ defined by

$$\mathcal{O}_{+,-}=\frac{i}{4}\bar{\psi}\sigma^{+1}(1-\gamma_5)\psi,$$

$$\mathcal{O}_{-,+}=-\frac{i}{4}\bar{\psi}\sigma^{+1}(1+\gamma_5)\psi.\qquad(9)$$

Using the reference frame where the momenta $\vec{p}$ and $\vec{p}'$ lie in the x-z plane, one can explicitly derive the following relations [2]:

$$A_{++,+-}=\epsilon\frac{\sqrt{t_0-t}}{2m}\left(\tilde{H}_T^q+(1-\zeta)\frac{E_T^q+\tilde{E}_T^q}{2}\right),$$

$$A_{-+,--}=\epsilon\frac{\sqrt{t_0-t}}{2m}\left(\tilde{H}_T^q+(1+\zeta)\frac{E_T^q-\tilde{E}_T^q}{2}\right),$$

$$A_{++,--}=\sqrt{1-\zeta^2}\left(H_T^q+\frac{t_0-t}{4m^2}\tilde{H}_T^q-\frac{\zeta^2}{1-\zeta^2}E_T^q+\frac{\zeta}{1-\zeta^2}\tilde{E}_T^q\right),$$

$$A_{-+,+-}=-\sqrt{1-\zeta^2}\frac{t_0-t}{4m^2}\tilde{H}_T^q,\qquad(10)$$

with $\epsilon=\mathrm{sgn}(D^1)$, where D^1 is the x component of $D^\alpha=P^+\Delta^\alpha-\Delta^+P^\alpha$ and $D^1=0$ corresponds to $t=t_0$. The minimum value of $-t$ for a given ζ is $-t_0=4m^2\zeta^2/(1-\zeta^2)$. Due to parity invariance one has the relation $A_{-\lambda'-,-\lambda+}=(-1)^{\lambda'-\lambda}A_{\lambda'+,\lambda-}$.

The chiral-odd GPDs are off-diagonal in the quark helicity basis but they can also be calculated in the transversity basis [3], which is more useful for the overlap formalism used in this work. Here we briefly discuss the transformation of matrix elements defining chiral-odd GPDs from the helicity basis to the transversity basis [3]. Consider the operators $\mathcal{O}_{+,-}+\mathcal{O}_{-,+}=-\frac{i}{2}\bar{\psi}\sigma^{+1}\gamma_5\psi$ and $\mathcal{O}_{+,-}-\mathcal{O}_{-,+}=\frac{i}{2}\bar{\psi}\sigma^{+1}\psi$ in the transversity basis, i.e.,

$$T_{\lambda'_t\lambda_t}^q=\left\langle p',\lambda'_t\right|\int\frac{dz^-}{2\pi}$$

$$\times e^{i\bar{x}P^+z^-}\bar{\psi}(-z/2)\gamma^+\gamma^1\gamma_5\psi(z/2)|p,\lambda_t\rangle,\qquad(11)$$

$$\tilde{T}_{\lambda'_t\lambda_t}^q=\left\langle p',\lambda'_t\right|\int\frac{dz^-}{2\pi}$$

$$\times e^{i\bar{x}P^+z^-}\frac{i}{2}\bar{\psi}(-z/2)\sigma^{+1}\psi(z/2)|p,\lambda_t\rangle,\qquad(12)$$

where λ_t (λ'_t) labels the transverse polarization of the initial (final) nucleon polarized along the +ve $x(\uparrow)$ or −ve $x(\downarrow)$ direction and the transverse basis states are defined as

$$|p,\uparrow\rangle=\frac{1}{\sqrt{2}}(|p,+\rangle+|p,-\rangle),\qquad(13)$$

$$|p,\downarrow\rangle=\frac{1}{\sqrt{2}}(|p,+\rangle-|p,-\rangle).\qquad(14)$$

These matrix elements obey the following relations as a result of parity invariance:

$$T_{\uparrow\uparrow}^q=-T_{\downarrow\downarrow}^q,\qquad T_{\uparrow\downarrow}^q=T_{\downarrow\uparrow}^q,$$
$$\tilde{T}_{\uparrow\uparrow}^q=\tilde{T}_{\downarrow\downarrow}^q,\qquad \tilde{T}_{\uparrow\downarrow}^q=-\tilde{T}_{\downarrow\uparrow}^q.\qquad(15)$$

We can now express them in terms of the matrix elements in the helicity basis as

$$T_{\uparrow\uparrow}^q=A_{++,--}+A_{-+,+-},\qquad T_{\uparrow\downarrow}^q=A_{++,+-}-A_{-+,--},$$
$$\tilde{T}_{\uparrow\uparrow}^q=A_{++,+-}+A_{-+,--},\qquad \tilde{T}_{\downarrow\uparrow}^q=A_{++,--}-A_{-+,+-}.$$
$$(16)$$

Finally, one can obtain the chiral-odd GPDs from the transverse matrix elements through the relations

$$H_T^q = \frac{1}{\sqrt{1-\zeta^2}} T_{\uparrow\uparrow}^q - \frac{2M\zeta}{\epsilon\sqrt{t_0-t}(1-\zeta^2)} T_{\uparrow\downarrow}^q, \quad (17)$$

$$E_T^q = \frac{2M}{\epsilon\sqrt{t_0-t}(1-\zeta^2)} (\zeta T_{\uparrow\downarrow}^q + \tilde{T}_{\uparrow\uparrow}^q)$$
$$- \frac{4M^2}{(t_0-t)\sqrt{1-\zeta^2}(1-\zeta^2)} (\tilde{T}_{\downarrow\uparrow}^q - T_{\uparrow\uparrow}^q), \quad (18)$$

$$\tilde{H}_T^q = \frac{2M^2}{(t_0-t)\sqrt{1-\zeta^2}} (\tilde{T}_{\downarrow\uparrow}^q - T_{\uparrow\uparrow}^q), \quad (19)$$

$$\tilde{E}_T^q = \frac{2M}{\epsilon\sqrt{t_0-t}(1-\zeta^2)} (T_{\uparrow\downarrow}^q + \zeta\tilde{T}_{\uparrow\uparrow}^q)$$
$$- \frac{4M^2\zeta}{(t_0-t)\sqrt{1-\zeta^2}(1-\zeta^2)} (\tilde{T}_{\downarrow\uparrow}^q - T_{\uparrow\uparrow}^q). \quad (20)$$

A. Overlap formalism

Using the overlap representation of light-front wave functions, we evaluate the chiral-odd GPDs in the light-front quark-diquark model. We restrict our discussion to the Dokshitzer-Gribov-Lipatov-Altarelli-Parisi (DGLAP) domain, i.e., $\zeta < x < 1$ where ζ is the skewness and x is the light-front longitudinal momentum fraction carried by the struck quark. This kinematical domain describes the diagonal $n \to n$ overlaps where the particle number remains conserved. This region corresponds to the situation where one removes a quark from the initial proton with light-front longitudinal momentum $(x+\zeta)P^+$ and reinserts it into the final proton with longitudinal momentum $(x-\zeta)P^+$. The diagonal $2 \to 2$ overlap representations of the matrix elements $T_{\lambda\lambda'}^q$ and $\tilde{T}_{\lambda\lambda'}^q$ in terms of light-front wave functions in the quark-diquark model are given by

$$T_{\uparrow\uparrow}^q = \int \frac{d^2\mathbf{k}_\perp}{16\pi^3} [\psi_{+q}^{+*}(x',\mathbf{k}_\perp')\psi_{-q}^-(x'',\mathbf{k}_\perp'') + \psi_{+q}^{-*}(x',\mathbf{k}_\perp')\psi_{-q}^+(x'',\mathbf{k}_\perp'')], \quad (21)$$

$$T_{\uparrow\downarrow}^q = \int \frac{d^2\mathbf{k}_\perp}{16\pi^3} [\psi_{+q}^{+*}(x',\mathbf{k}_\perp')\psi_{-q}^+(x'',\mathbf{k}_\perp'') - \psi_{+q}^{-*}(x',\mathbf{k}_\perp')\psi_{-q}^-(x'',\mathbf{k}_\perp'')], \quad (22)$$

$$\tilde{T}_{\uparrow\uparrow}^q = \int \frac{d^2\mathbf{k}_\perp}{16\pi^3} [\psi_{+q}^{+*}(x',\mathbf{k}_\perp')\psi_{-q}^+(x'',\mathbf{k}_\perp'') + \psi_{+q}^{-*}(x',\mathbf{k}_\perp')\psi_{-q}^-(x'',\mathbf{k}_\perp'')], \quad (23)$$

$$\tilde{T}_{\uparrow\downarrow}^q = \int \frac{d^2\mathbf{k}_\perp}{16\pi^3} [\psi_{+q}^{+*}(x',\mathbf{k}_\perp')\psi_{-q}^-(x'',\mathbf{k}_\perp'') - \psi_{+q}^{-*}(x',\mathbf{k}_\perp')\psi_{-q}^+(x'',\mathbf{k}_\perp'')], \quad (24)$$

where, for the final struck quark

$$x' = \frac{x-\zeta}{1-\zeta}, \qquad \mathbf{k}_\perp' = \mathbf{k}_\perp + (1-x')\frac{\mathbf{\Delta}_\perp}{2}, \quad (25)$$

and for the initial struck quark

$$x'' = \frac{x+\zeta}{1+\zeta}, \qquad \mathbf{k}_\perp'' = \mathbf{k}_\perp - (1-x'')\frac{\mathbf{\Delta}_\perp}{2}. \quad (26)$$

The explicit calculation of the matrix elements $T_{\lambda\lambda'}^q$ and $\tilde{T}_{\lambda\lambda'}^q$ using the light-front wave functions of the quark-diquark model given in Eq. (4) gives

$$T_{\uparrow\uparrow}^q = \frac{1}{\kappa^2} \left[\frac{\log x' \log x''}{(1-x')(1-x'')}\right]^{1/2} \left[(N_q^{(1)})^2 (x'x'')^{a_q^{(1)}} \{(1-x')(1-x'')\}^{b_q^{(1)}} \frac{1}{A} - (N_q^{(2)})^2 \frac{1}{M_n^2} (x'x'')^{a_q^{(2)}-1} \{(1-x')(1-x'')\}^{b_q^{(2)}} \right.$$
$$\left. \times \left(\frac{B^2}{4A^2} - \frac{1}{4}(1-x')(1-x'') + \frac{B}{4A}(x''-x')\right) \frac{Q^2}{A}\right] \exp\left[Q^2\left(C - \frac{B^2}{4A}\right)\right], \quad (27)$$

$$T_{\uparrow\downarrow}^q = -\frac{N_q^{(1)}N_q^{(2)}}{\kappa^2} \left[\frac{\log x' \log x''}{(1-x')(1-x'')}\right]^{1/2} \frac{1}{M_n} \left[(x')^{a_q^{(1)}}(1-x')^{b_q^{(1)}}(x'')^{a_q^{(2)}-1}(1-x'')^{b_q^{(2)}} \times \left(\frac{BQ}{2A^2} - \frac{Q}{2A}(1-x'')\right)\right.$$
$$\left. + (x')^{a_q^{(2)}-1}(1-x')^{b_q^{(2)}}(x'')^{a_q^{(1)}}(1-x'')^{b_q^{(1)}}\left(\frac{BQ}{2A^2} + \frac{Q}{2A}(1-x'')\right)\right] \exp\left[Q^2\left(C - \frac{B^2}{4A}\right)\right], \quad (28)$$
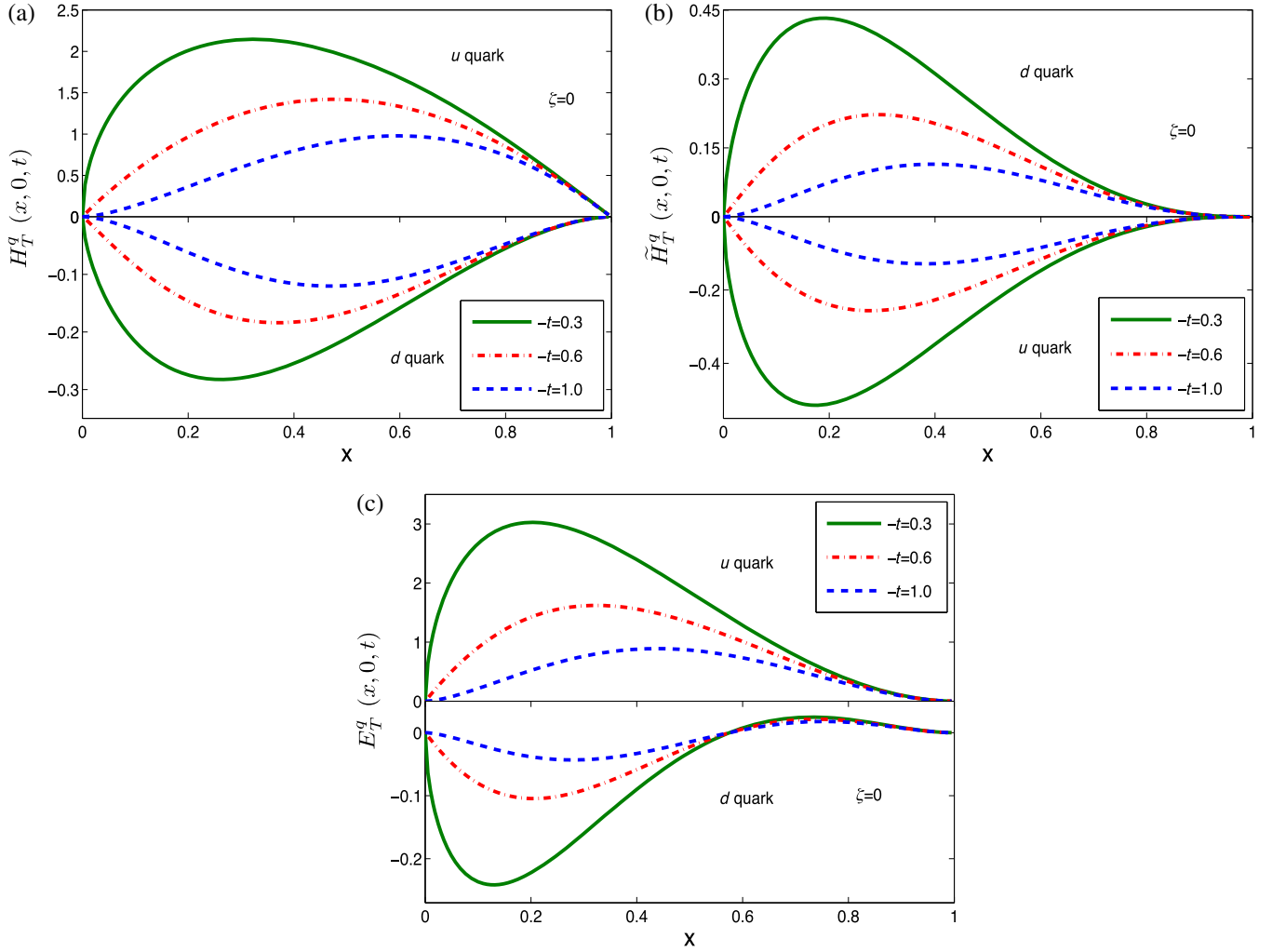
FIG. 1 (color online).   Plots of the chiral-odd GPDs for zero skewness vs x and different values of $-t$ in GeV^2 for u and d quarks.

$$\tilde{T}^q_{\uparrow\uparrow} = -\frac{N^{(1)}_q N^{(2)}_q}{\kappa^2}\left[\frac{\log x' \log x''}{(1-x')(1-x'')}\right]^{1/2}\frac{1}{M_n}\left[(x')^{a^{(1)}_q}(1-x')^{b^{(1)}_q}(x'')^{a^{(2)}_q-1}(1-x'')^{b^{(2)}_q}\left(\frac{BQ}{2A^2}-\frac{Q}{2A}(1-x'')\right)\right.$$

$$\left.- (x')^{a^{(2)}_q-1}(1-x')^{b^{(2)}_q}(x'')^{a^{(1)}_q}(1-x'')^{b^{(1)}_q}\left(\frac{BQ}{2A^2}+\frac{Q}{2A}(1-x'')\right)\right]\exp\left[Q^2\left(C-\frac{B^2}{4A}\right)\right], \tag{29}$$

$$\tilde{T}^q_{\uparrow\downarrow} = \frac{1}{\kappa^2}\left[\frac{\log x' \log x''}{(1-x')(1-x'')}\right]^{1/2}\left[(N^{(1)}_q)^2(x'x'')^{a^{(1)}_q}\{(1-x')(1-x'')\}^{b^{(1)}_q}\frac{1}{A}+(N^{(2)}_q)^2\frac{1}{M^2_n}(x'x'')^{a^{(2)}_q-1}\{(1-x')(1-x'')\}^{b^{(2)}_q}\right.$$

$$\left.\times\left(\frac{B^2}{4A^2}-\frac{1}{4}(1-x')(1-x'')+\frac{B}{4A}(x''-x')\right)\frac{Q^2}{A}\right]\exp\left[Q^2\left(C-\frac{B^2}{4A}\right)\right], \tag{30}$$

where $\Delta^2_\perp = Q^2 = -t(1-\zeta^2)-4M^2_n\zeta^2$. A, B, and C are functions of x and ζ,

$$A = A(x,\zeta) = -\frac{\log x'}{2\kappa^2(1-x')^2}-\frac{\log x''}{2\kappa^2(1-x'')^2},$$

$$B = B(x,\zeta) = \frac{\log x'}{2\kappa^2(1-x')}-\frac{\log x''}{2\kappa^2(1-x'')},$$

$$C = C(x,\zeta) = \frac{1}{4}\left[\frac{\log x'}{2\kappa^2}+\frac{\log x''}{2\kappa^2}\right]. \tag{31}$$
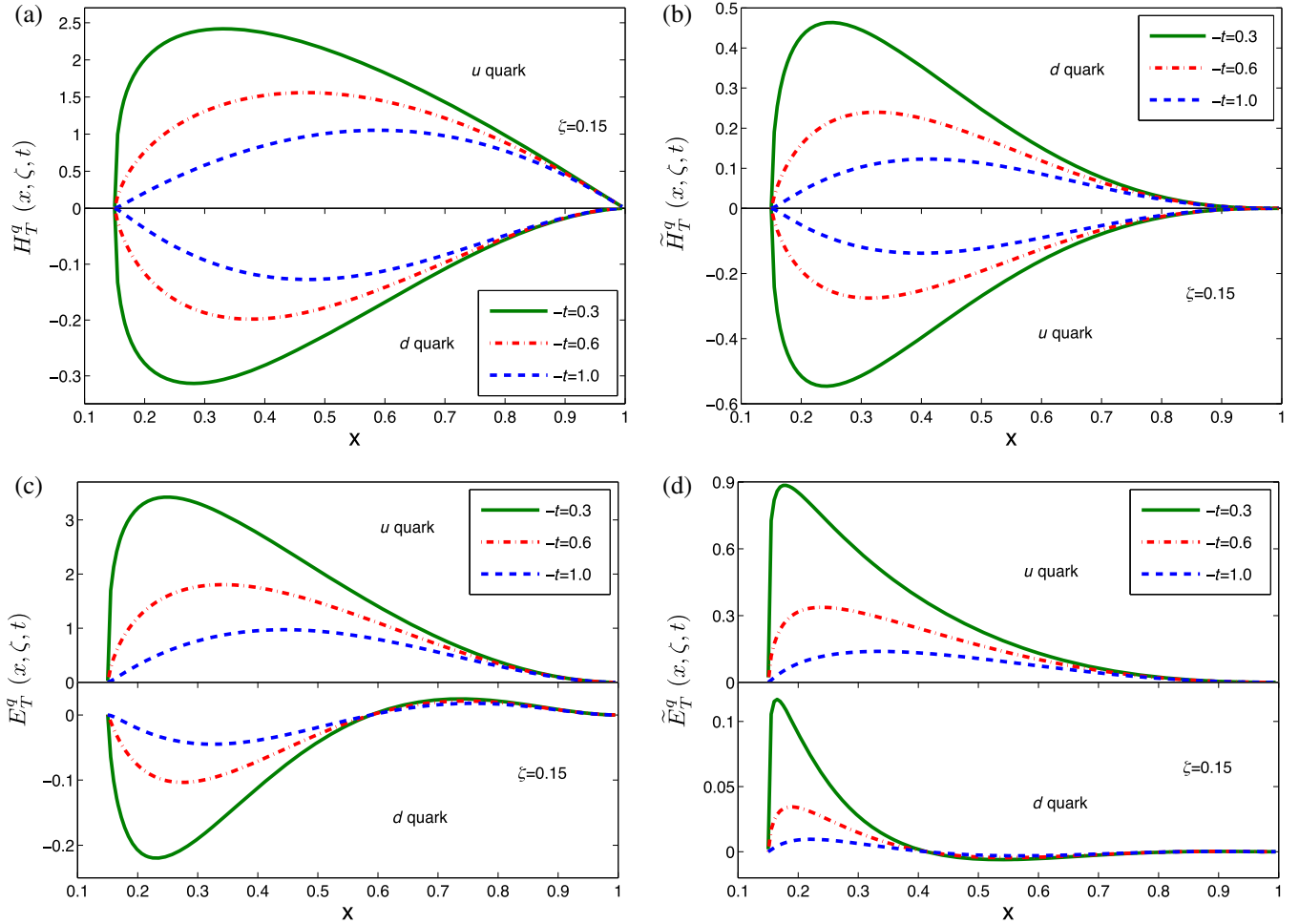
FIG. 2 (color online).   Plots of chiral-odd GPDs for nonzero skewness vs x and different values of $-t$ in GeV^2, for a fixed value of $\zeta = 0.15$. (a) H_T^q. (b) $\tilde{H}_T^q$. (c) E_T^q. (d) $\tilde{E}_T^q$. q stands for u and d quarks.

Using the matrix elements calculated in Eqs. (27)–(30) we evaluate the chiral-odd GPDs in Eqs. (17)–(20). All the GPDs are suitably scaled by the flavor factors P_q, where $P_u = \frac{4}{3}$ and $P_d = -\frac{1}{3}$ are dictated by SU(6) spin-flavor symmetry [34].

In Fig. 1 we show the t dependence of chiral-odd GPDs H_T^q, $\tilde{H}_T^q$, and E_T^q for up and down quarks in the quark-diquark model when the skewness $\zeta = 0$. Being an odd function of ζ, the GPD $\tilde{E}_T^q$ vanishes at $\zeta = 0$ in this model. Similar behavior for $\tilde{E}_T^q$ has been reported in Refs. [2,3]. One can notice that the signs of all three GPDs for the u quark are opposite those of the d quark and $\tilde{H}_T^q$ has the opposite sign as $H_T^q(x, 0, t)$, as expected from SU(6) symmetry. The peaks of all the distributions move to higher values of x as $-t$ increases. For $\zeta \neq 0$, all four GPDs are shown in Figs. 2 and 3. In Fig. 2 the GPDs are shown for a fixed value of $\zeta = 0.15$ but for different values of $-t$. In Fig. 3, we plot the GPDs for a fixed value of $-t = 0.7$ GeV^2 and different values of ζ. One can notice

that the heights of the peaks of the distributions increase and shift to higher x with increasing ζ for fixed $-t$. In all cases, the GPDs vanish at $x = \zeta$. The reason for this is that in our approach we consider only the contribution from the valence quarks. In this model we cannot evaluate the total (sea + valence) GPDs as the model itself depends only on the valence quarks. Similar behavior for the chiral-odd GPDs was found in the relativistic constituent quark model calculated in Ref. [3]. Also, the region for $x < \zeta$ (the so-called Efremov-Radyushkin-Brodsky-Lepage region) where quark-antiquark pair creation/annihilation is involved is not included in this model. In Fig. 4, we show the GPDs as functions of ζ for different values of $-t$ and fixed x. It can be noticed that only $\tilde{E}_T^q(x, \zeta, t)$ [Figs. 4(g) and 4(h)] shows markedly different behavior from the other GPDs. $\tilde{E}_T^q(x, \zeta, t)$ rises smoothly from zero as ζ increases for all t values, whereas the other GPDs have different values at $\zeta = 0$ for different values of $-t$. Similar behavior for the chiral-odd GPDs has been observed [9] in a QED model.
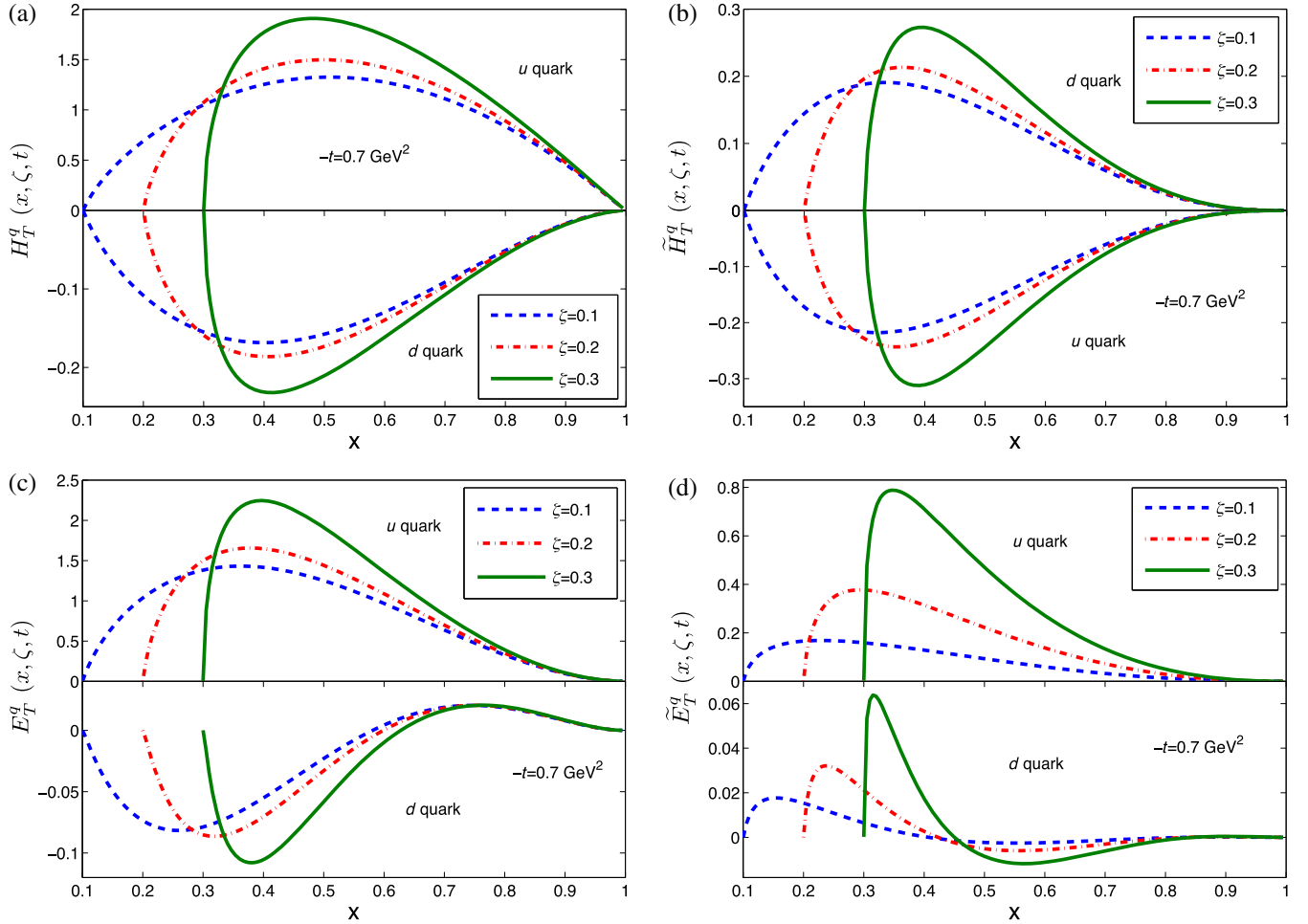
FIG. 3 (color online).   Plots of chiral-odd GPDs for nonzero skewness vs x and different values of ζ, for a fixed value of $t = 0.7$ GeV^2.
(a) H_T^q. (b) $\tilde{H}_T^q$. (c) E_T^q. (d) $\tilde{E}_T^q$. q stands for u and d quarks.

B. Mellin moments of chiral-odd GPDs

The Mellin moments of the valence GPDs are defined as

$$H_{Tn0}^q(t) = \int_0^1 dx\, x^{n-1} H_T^q(x,0,t), \qquad (32)$$

where the index $n = 1, 2, 3$ etc., and the second subscript indicates that the moments are evaluated at zero skewness. The moments of the other GPDs $E_{Tn0}^q(t)$ and $\tilde{H}_{Tn0}^q(t)$ can also be defined in the same way as Eq. (32). The first moments of chiral-odd GPDs give the tensor form factors. The forward values, $t = 0$, of the form factor $g_T = H_{T10}(t = 0)$ can be identified as the tensor charge [23]. The combination of tensor form factors $\bar{E}_{T10}^q = (E_{T10}^q + 2\tilde{H}_{T10}^q)$ in the forward limit plays a role very similar to that of the anomalous magnetic moment κ^q and therefore may be identified with a tensor magnetic moment, $\kappa_T^q = \bar{E}_{T10}^q(t = 0)$ [5]. In Fig. 5, we compare our result for the tensor form factors with the corresponding results from the

lattice [22] and the chiral quark-soliton model [35,36]. The tensor form factors for the u quark in this model agree well with the chiral quark-soliton model (χQSM) but both (this model and the χQSM model) deviate from lattice results for both u and d quarks. The second moments of these GPDs correspond to the gravitational form factors of quarks with transverse spin in an unpolarized nucleon. A linear combination of $H_{T20}^q(t)$, $E_{T20}^q(t)$, and $\tilde{H}_{T20}^q(t)$ gives the angular momentum carried by quarks with transverse spin in an unpolarized nucleon [5], in analogy with Ji's angular momentum sum rule. The third moments of the GPDs generate form factors of a twist-two operator having two covariant derivatives [1] and the higher-order moments give the form factors of higher-twist operators.

In Fig. 6 we show the first three moments of the chiral-odd GPDs $|t|H_{Tn0}^q(t)$, $|t|E_{Tn0}^q(t)$, and $|t|\tilde{H}_{Tn0}^q(t)$ as functions of $\sqrt{-t}$ for u and d quarks. We find a strong decrease in the magnitudes of the moments with increasing n. This can be understood from the behavior of the GPDs with x as
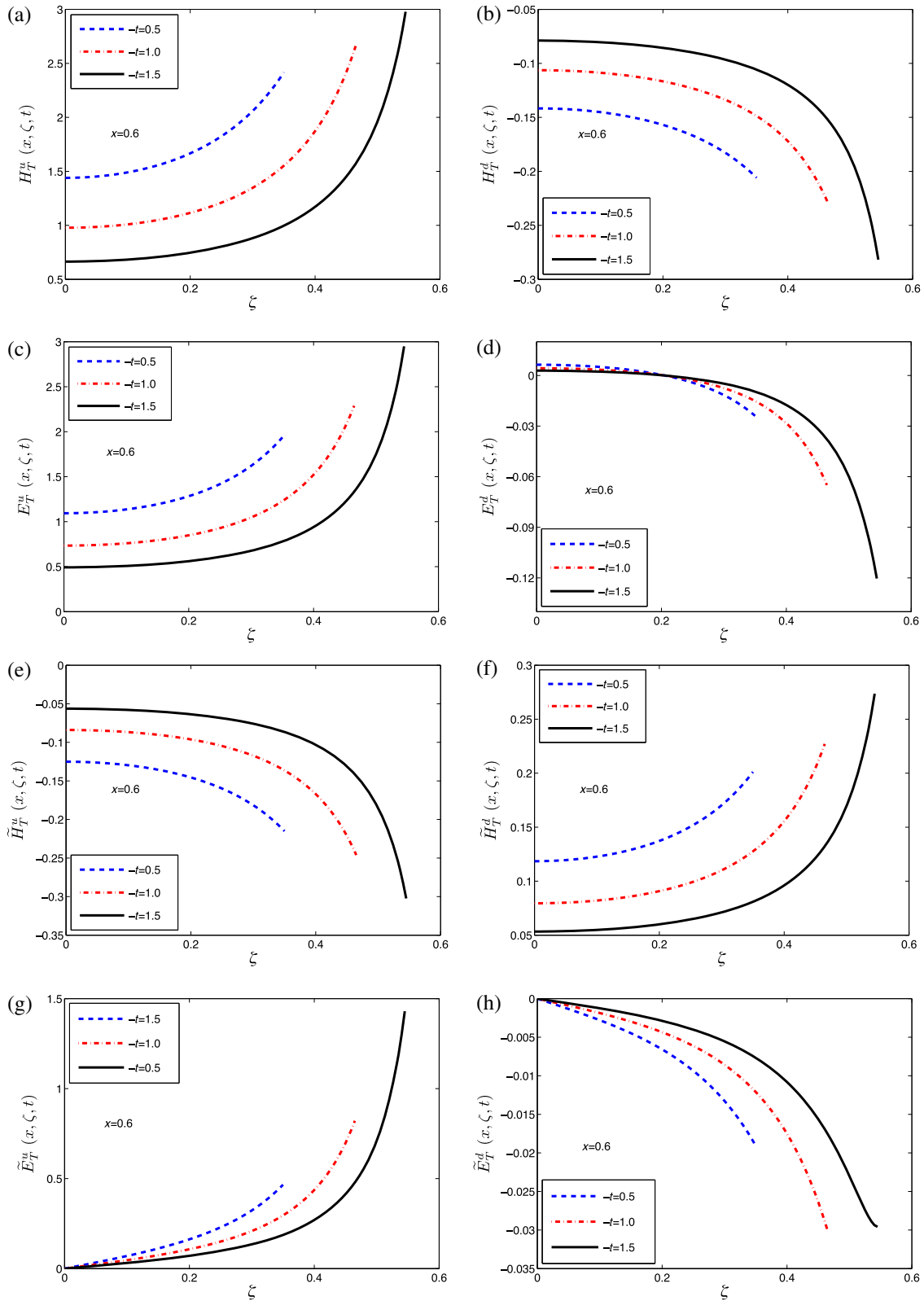
FIG. 4 (color online).   Plots of chiral-odd GPDs for nonzero skewness vs ζ and different values of $-t$ in GeV^2, for a fixed value of $x = 0.6$. The left panel is for the u quark and the right panel is for the d quark.
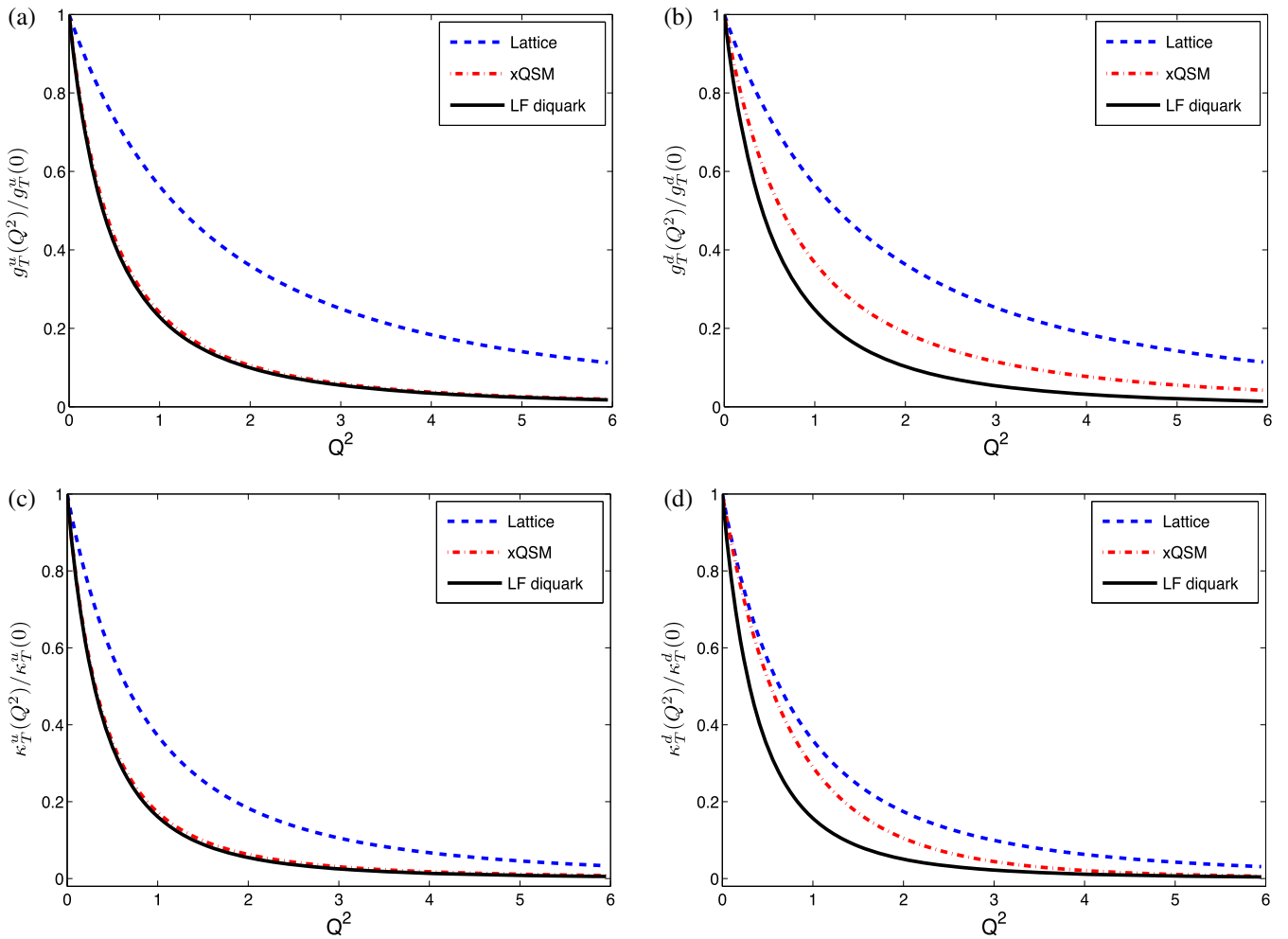
FIG. 5 (color online). Tensor form factors for u and d quarks are compared with the lattice [22] and chiral quark-soliton model (xQSM) [35,36] results.

shown in Fig. 1. Higher moments involve higher powers of x and hence the dominant contributions come from the large-x region($x \to 1$), but the GPDs decrease rapidly as x increases, and hence the higher moments become smaller. We also observe that as the index n increases, the decrease of the moments becomes slower with increasing $-t$. This again can be explained in terms of the decrease of the GPDs with the momentum fraction x, which results in a weaker t slope for the higher moments. Similar behavior has been observed in lattice QCD calculations of the moments of chiral-odd GPDs [22].

IV. IMPACT PARAMETER REPRESENTATION OF CHIRAL-ODD GPDs

GPDs in transverse impact parameter space are defined by a two-dimensional Fourier transform in $\Delta_\perp$ as follows [6,7]:

$$H_T(x,\zeta,b_\perp) = \frac{1}{(2\pi)^2} \int d^2\Delta_\perp e^{-i\Delta_\perp \cdot b_\perp} H_T(x,\zeta,t), \quad (33)$$

$$E_T(x,\zeta,b_\perp) = \frac{1}{(2\pi)^2} \int d^2\Delta_\perp e^{-i\Delta_\perp \cdot b_\perp} E_T(x,\zeta,t), \quad (34)$$

$$\tilde{H}_T(x,\zeta,b_\perp) = \frac{1}{(2\pi)^2} \int d^2\Delta_\perp e^{-i\Delta_\perp \cdot b_\perp} \tilde{H}_T(x,\zeta,t), \quad (35)$$

$$\tilde{E}_T(x,\zeta,b_\perp) = \frac{1}{(2\pi)^2} \int d^2\Delta_\perp e^{-i\Delta_\perp \cdot b_\perp} \tilde{E}_T(x,\zeta,t). \quad (36)$$

Here, $b_\perp$ is the transverse impact parameter conjugate to $\Delta_\perp$. For zero skewness, $\mathbf{b}_\perp$ gives a measure of the transverse distance between the struck parton and the center of momentum of the hadron. $b_\perp$ satisfies the condition $\sum_i x_i b_{\perp i} = 0$, where the sum is over the number of partons. The relative distance between the struck parton and the center of momentum of the spectator system is given by $\frac{|\mathbf{b}_\perp|}{1-x}$, which provides us with an estimate of the size of the bound state [37]. In the DGLAP region $x > \zeta$, the impact parameter $b_\perp$ implies the location where the quark is pulled out and reinserted into the nucleon. In
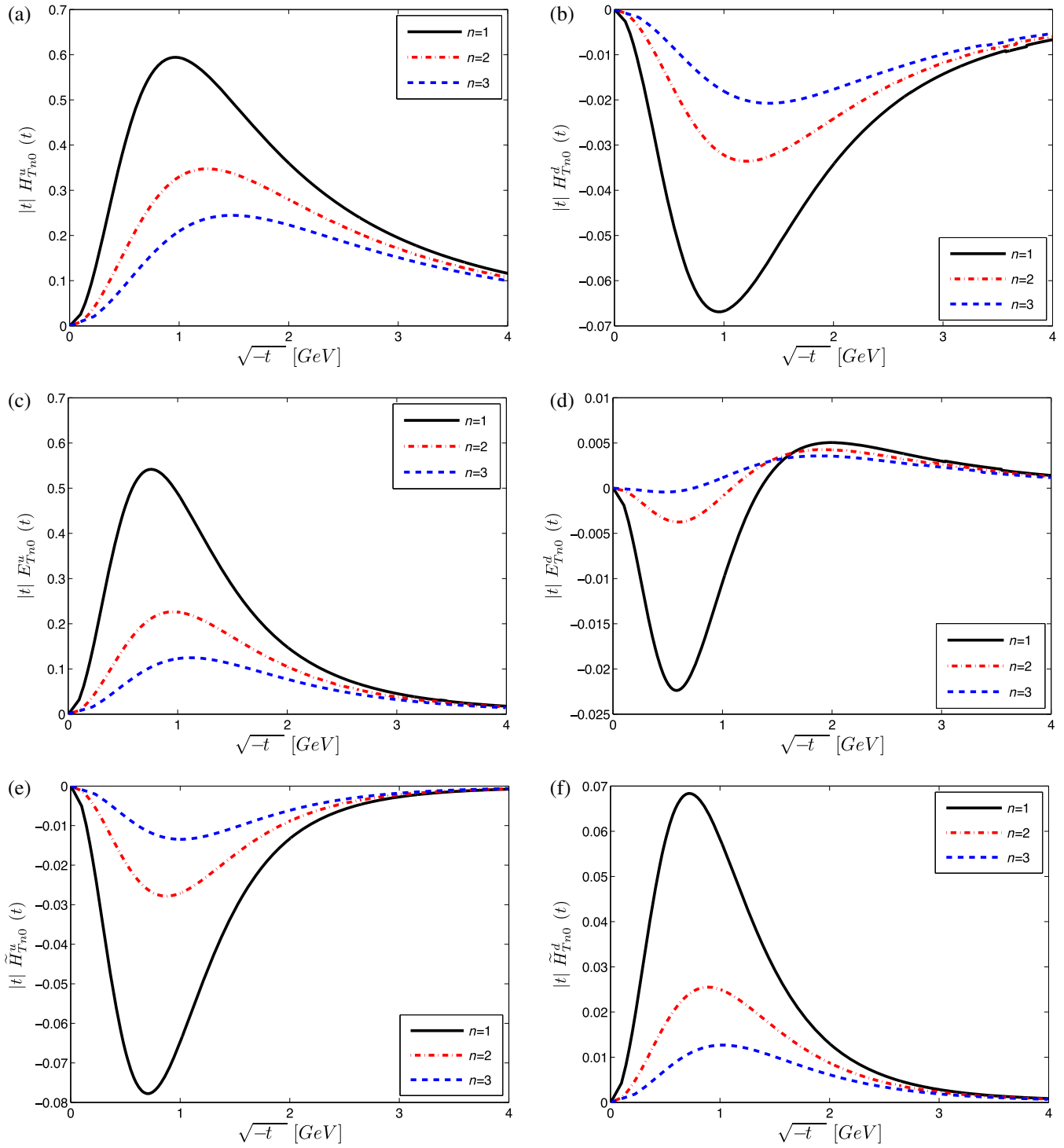
FIG. 6 (color online). Plots of the first three moments of the chiral-odd GPDs for zero skewness vs $\sqrt{-t}$ in GeV. The left panel is for the u quark and the right panel is for the d quark.

the Efremov-Radyushkin-Brodsky-Lepage domain $x < \zeta$, $b_\perp$ provides the transverse distance of the quark-antiquark pair inside the nucleon. For zero skewness, the chiral-odd GPDs also have a density interpretation in transverse impact parameter space like chiral-even GPDs

depending on the polarization of both the active quark and the nucleon. A combination of $E_T(x, b_\perp)$ and $\tilde{H}_T(x, b_\perp)$ $(E_T + 2\tilde{H}_T)$ is responsible for a deformation in the transversity asymmetry quarks in an unpolarized target [4,5,10]. This is similar to the role played by

$E(x, b_\perp)$ for both the unpolarized active quark and the nucleon. On the other hand, a combination of $H_T(x, b_\perp)$ and $\tilde{H}_T(x, b_\perp)$ provides a distortion in the transverse spin density when the active quark and the nucleon are transversely polarized [4,38]. Note that the density interpretation is possible only in the limit $\zeta = 0$, but in most experiments ζ is nonzero. So, it is interesting to investigate the chiral-odd GPDs in the impact parameter space with nonzero ζ.

We show the skewness-dependent chiral-odd GPDs in transverse impact parameter space for fixed $\zeta = 0.2$ as functions of $b = |b_\perp|$ and x for u and d quarks in Fig. 7. Similarly, all the chiral-odd GPDs as functions of ζ and b for a fixed value of $x = 0.6$ are shown in Fig. 8. The peak of the distribution $H_T(x, \zeta, b_\perp)$ for fixed ζ appears at lower x for the d quark and shifts to higher x for the u quark, while for $\tilde{H}_T(x, \zeta, b_\perp)$ we get the peak at lower x for both u and d quarks. For both $E_T(x, \zeta, b_\perp)$ and $\tilde{E}_T(x, \zeta, b_\perp)$, the peaks arise at lower x for both u and d quarks but we also get an oscillatory behavior for both GPDs of the d quark. This is due to the fact that $E_T^d(x, \zeta, t)$ and $\tilde{E}_T^d(x, \zeta, t)$ have slight oscillatory behavior, as can be seen in Fig. 2(c) and 2(d). Except for $\tilde{H}_T(x, \zeta, b_\perp)$, the peaks of the u quark in all other distributions are sufficiently large compared to the d quark. For $\tilde{H}_T(x, \zeta, b_\perp)$, the peak of the u quark is slightly larger compared to the d quark. For small b, $\tilde{E}_T(x, \zeta, b_\perp)$ falls off slowly at large x for the u quark compared to the d quark. With increasing x, the width of all the distributions in transverse impact parameter space decreases, which implies that the distributions are more localized near the center of momentum for higher values of x. Substantial differences are observed in $\tilde{E}_T(x, \zeta, b_\perp)$ from other GPDs when the GPDs are plotted against ζ and b for fixed values of x in Fig. 8. $\tilde{E}_T(x, \zeta, b_\perp)$ increases with increasing ζ. Another interesting behavior of all the GPDs is that the peaks of all the distributions become broader as ζ increases for a fixed value of x. This means that as the momentum transfer in the longitudinal direction increases the probability of hitting the transversely polarized active quark at a larger transverse impact parameter b increases.

A. GPDs in longitudinal impact parameter space

The boost-invariant longitudinal impact parameter is defined as $\sigma = \frac{1}{2} b^- P^+$ which is conjugate to ζ, the measure of longitudinal momentum transfer. The parameter σ was first introduced in Ref. [11]. The DVCS amplitude in a QED model of a dressed electron shows an interesting diffraction pattern in the longitudinal impact parameter space analogous to diffractive scattering of a wave in optics [11]. In analogy with optics, the finite size of ζ can be interpreted as a slit of finite width that produces the diffraction pattern. It should be mentioned here that the FT with a finite range of ζ

of any function does not show the diffraction pattern [12]. The pattern depends on the behavior of the function. The chiral-odd GPDs calculated in Ref. [9] for a simple relativistic spin-half system of an electron dressed with a photon exhibit a similar diffraction pattern in the longitudinal impact parameter space. A phenomenological model for proton GPDs shows a similar diffraction pattern [12]. Similar diffraction patterns are also observed for the chiral-even GPDs in this light-front quark-diquark model [14] as well as in the QED model [13]. The GPDs in longitudinal position space are defined as

$$H_T(x, \sigma, t) = \frac{1}{2\pi} \int_0^{\zeta_f} d\zeta e^{i\zeta P^+ b^-/2} H_T(x, \zeta, t)$$
$$= \frac{1}{2\pi} \int_0^{\zeta_f} d\zeta e^{i\zeta\sigma} H_T(x, \zeta, t), \qquad (37)$$

$$E_T(x, \sigma, t) = \frac{1}{2\pi} \int_0^{\zeta_f} d\zeta e^{i\zeta P^+ b^-/2} E_T(x, \zeta, t)$$
$$= \frac{1}{2\pi} \int_0^{\zeta_f} d\zeta e^{i\zeta\sigma} E_T(x, \zeta, t). \qquad (38)$$

Similarly, one can obtain $\tilde{H}_T(x, \sigma, t)$ and $\tilde{E}_T(x, \sigma, t)$ as well. Since we are considering the region $\zeta < x < 1$, the upper limit of ζ integration ζ_f is given by x if x is smaller than ζ_{max}; otherwise, it is given by ζ_{max} if x is larger than ζ_{max} where the maximum value of ζ for a fixed $-t$ is given by

$$\zeta_{max} = \sqrt{\frac{(-t)}{(-t + 4M_n^2)}}. \qquad (39)$$

We show the Fourier spectrum of all the chiral-odd GPDs for u and d quarks in longitudinal position space as a function of σ for fixed $x = 0.3$ and different values of $-t$ in Fig. 9. H_T^q, E_T^q, and $\tilde{H}_T^q$ display a diffraction pattern in σ space as observed for the DVCS amplitude in Ref. [11], but $\tilde{E}_T^q(x, \sigma, t)$ does not show the same pattern. This is due to the distinctly different behavior of $\tilde{E}_T^q(x, \zeta, t)$ with ζ compared to the other GPDs. This again shows that the diffraction pattern is not solely due to the finiteness of ζ integration: the functional forms of the GPDs are also crucial. For all the diffraction patterns the first minima appear at the same values of σ. We also show the chiral-odd GPDs in σ space for fixed $-t = 0.4$ GeV^2 and different values of x in Fig. 10. Analogously to the single-slit optical diffraction pattern, here ζ_{max} plays the role of the slit width. Since the position of the minima are inversely proportional to the slit width, the minima move towards the center of the diffraction pattern as the slit width ζ_{max} increases.
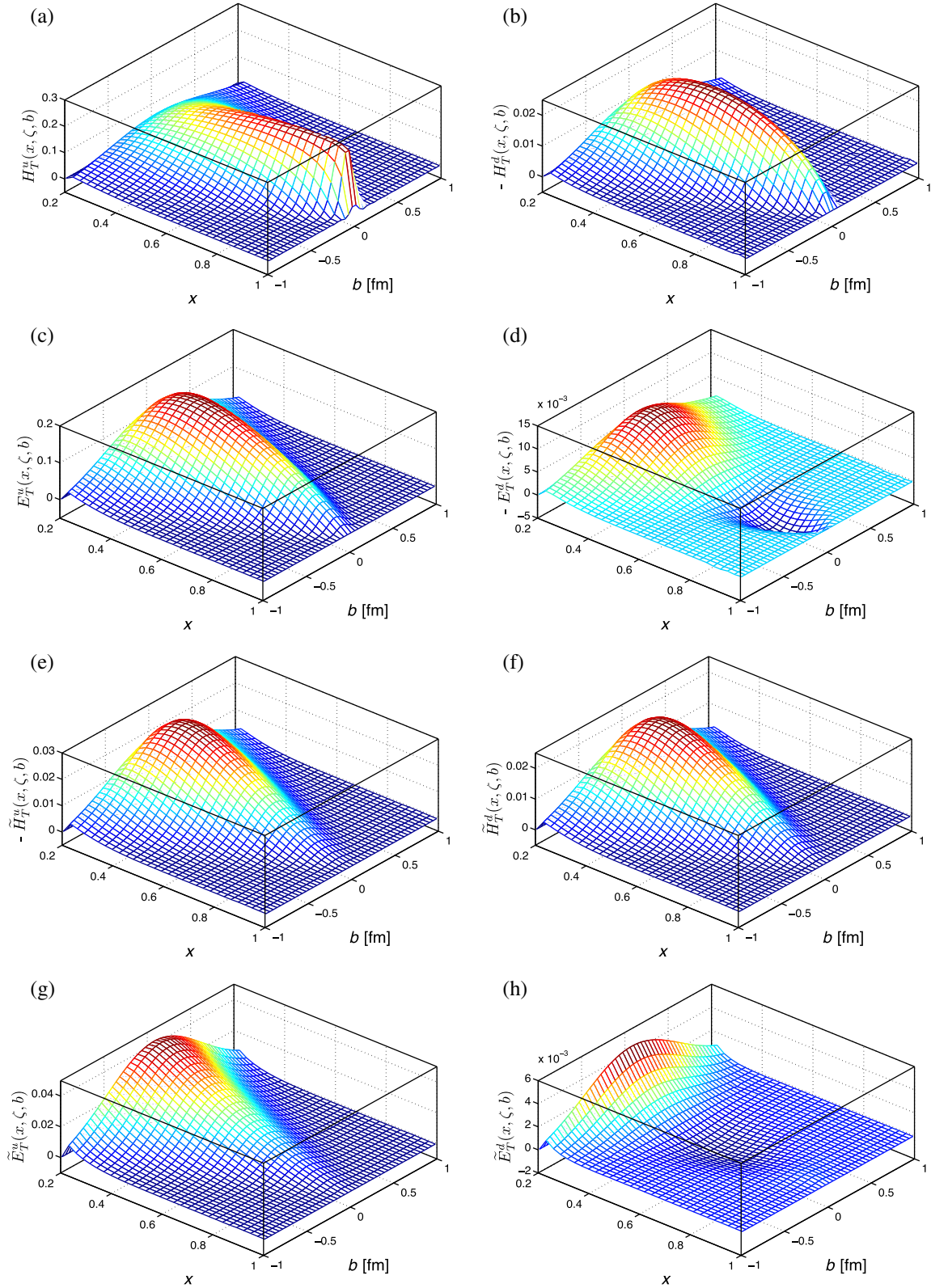
FIG. 7 (color online).   Plots of chiral-odd GPDs for nonzero skewness in impact space vs x and $b = |\mathbf{b}|$ for a fixed value of $\zeta = 0.2$. The left panel is for the u quark and the right panel is for the d quark.
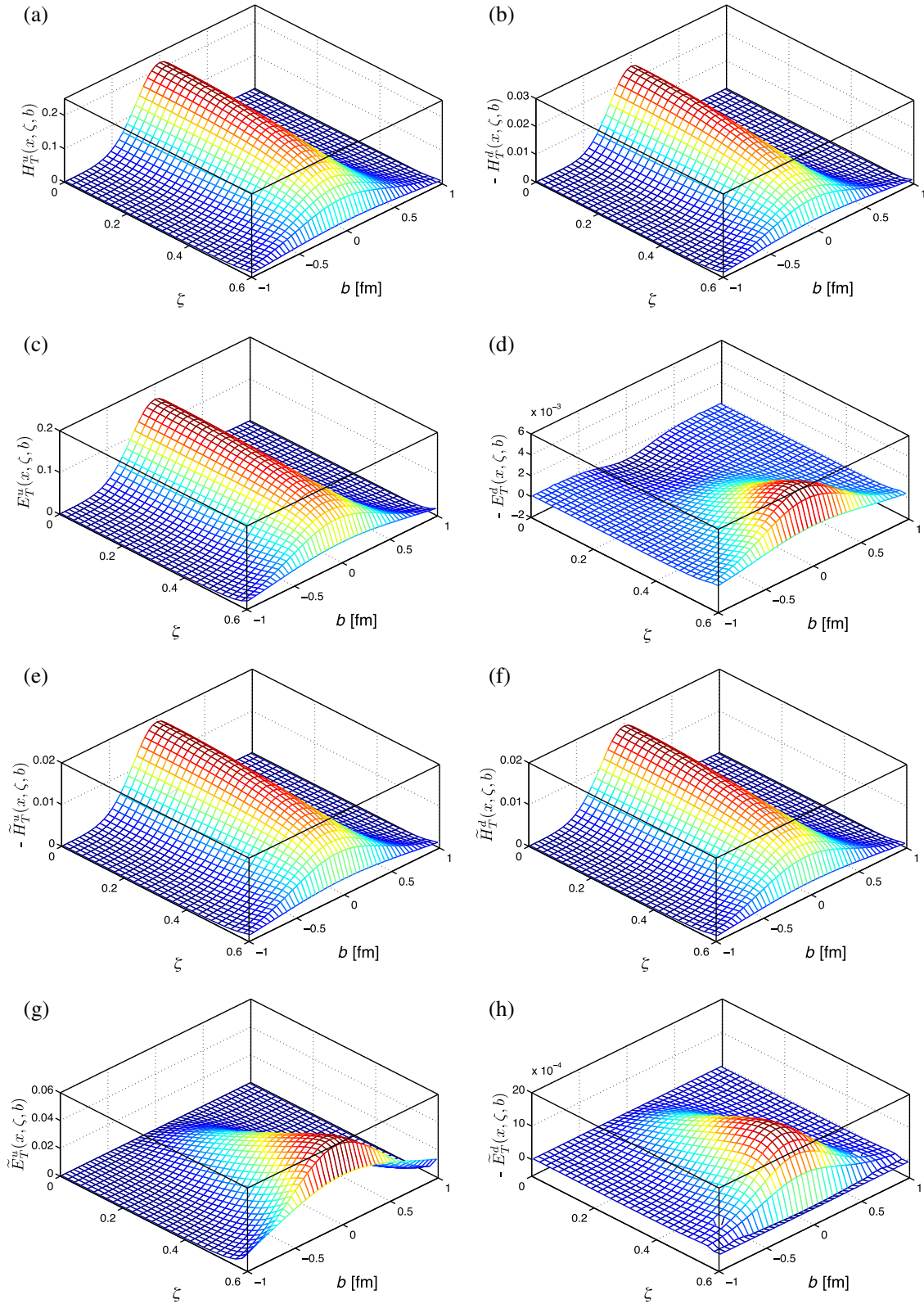
FIG. 8 (color online).   Plots of chiral-odd GPDs for nonzero skewness in impact space vs ζ and $b = |\mathbf{b}|$ for a fixed value of $x = 0.6$. The left panel is for the u quark and the right panel is forthe d quark.
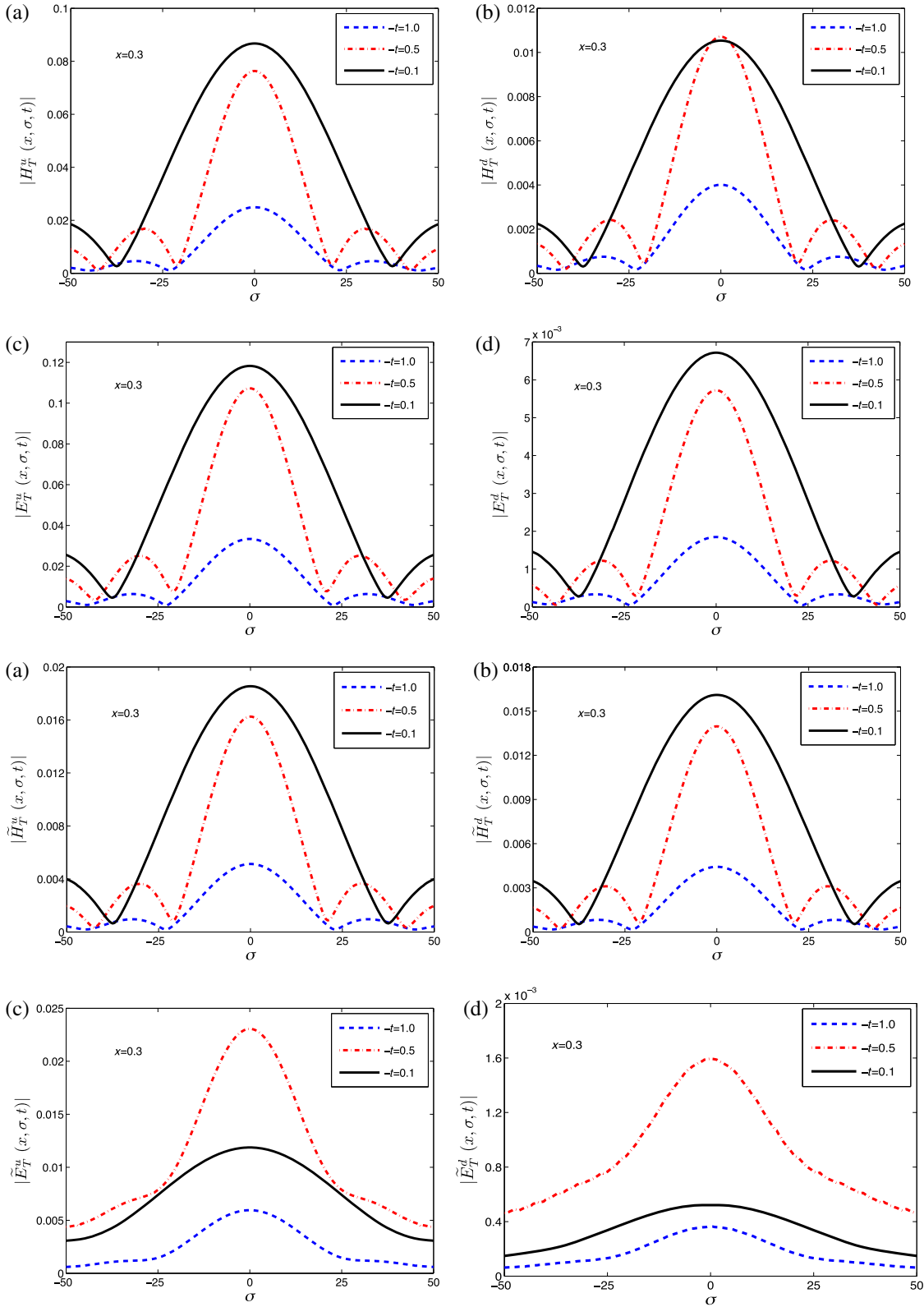
FIG. 9 (color online).   Plots of the chiral-odd GPDs in longitudinal impact space vs σ and different values of $-t$ in GeV^2, for a fixed value of $x = 0.3$. The left panel is for the u quark and the right panel is for the d quark.
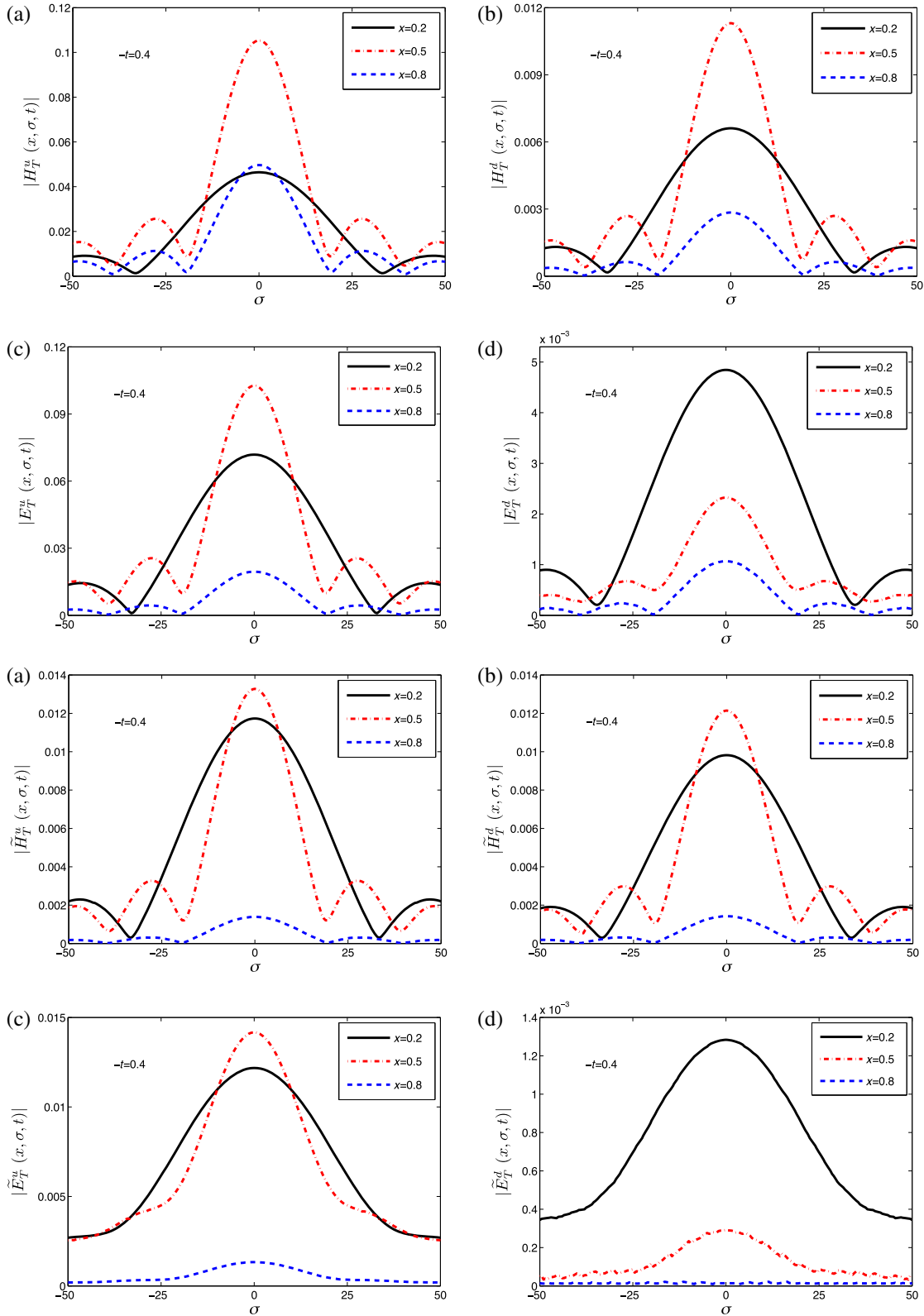
FIG. 10 (color online). Plots of the chiral-odd GPDs in longitudinal impact space vs σ and different values of x, for a fixed value of $-t = 0.4$ GeV^2. The left panel is for the u quark and the right panel is for the d quark.

V. SUMMARY

We have investigated the chiral-odd GPDs for the u and d quarks in the proton for both zero and nonzero skewness in the light-front quark-diquark model predicted by the soft-wall AdS/QCD. We have found that $\tilde{E}_T^q(x, 0, t)$ is zero in this model because it is an odd function of ζ. $\tilde{H}_T^q$ has the opposite sign as H_T^q for both u and d quarks as expected from SU(6). For zero skewness, all the chiral-odd GPDs for the u quark are opposite those of the d quark. We have calculated the GPDs for nonzero skewness in the DGLAP region, i.e., for $(x > \zeta)$. The peaks of the distributions move to higher values of x for fixed ζ with an increase of $-t$, similar to the case of $\zeta = 0$. The heights of the peaks increase and also shift to higher values of x as ζ increases for fixed $-t$. We observed markedly different behavior for $\tilde{E}_T^q$ compared to the other chiral-odd GPDs when we plot the GPDs against ζ for fixed x and different $-t$. We saw that as ζ increases, $\tilde{E}_T^q$ starts to increase smoothly from zero but other GPDs rise from different values at $\zeta = 0$ for different values of $-t$.

We have also presented all the chiral-odd GPDs in the transverse position, impact parameter (b), and longitudinal position (σ) spaces by taking the FT of the GPDs with respect to the transverse momentum transfer ($\Delta_\perp$) and ζ,

respectively. The impact parameter b gives a measure of the transverse distance between the struck parton and the center of momentum of the hadron. In this model (except for $\tilde{H}_T^q$), the behavior of the GPDs in the transverse impact parameter space for u and d quarks are quite different when plotted in x and b. Except for the magnitude, the natures of H_T^q, E_T^q, and $\tilde{H}_T^q$ are more or less the same when plotted against ζ and b, but $\tilde{E}_T^q$ shows a different behavior. The widths of all the distributions increase with increasing ζ and decreasing x. We found that the GPDs H_T, E_T, and $\tilde{H}_T$ for u and d quarks in σ space show diffraction patterns analogous to the diffractive scattering of a wave in optics. A similar diffraction pattern has also been observed in some other models. The qualitative nature of the diffraction patterns for all three chiral-odd GPDs are the same for both u and d quarks. The general features of this pattern are mainly dependent on the finiteness of the ζ integration as well as the dependence of the GPDs on x, ζ, and t. Like other GPDs, $\tilde{E}_T$ does not show the diffraction pattern. This is due to a different dependence of $\tilde{E}_T$ on ζ compared to the other GPDs. It also indicates that the diffraction pattern is not solely due to the finiteness of the ζ integration and that the functional behaviors of the GPDs are important in order to have the diffraction pattern.

[1] For reviews on generalized parton distributions and DVCS see M. Diehl, Phys. Rep. **388**, 41 (2003); A. V. Belitsky and A. V. Radyushkin, Phys. Rep. **418**, 1 (2005); K. Goeke, M. V. Polyakov, and M. Vanderhaeghen, Prog. Part. Nucl. Phys. **47**, 401 (2001).

[2] M. Diehl, Eur. Phys. J. C **19**, 485 (2001).

[3] B. Pasquini, M. Pincetti, and S. Boffi, Phys. Rev. D **72**, 094029 (2005).

[4] M. Diehl and P. Hagler, Eur. Phys. J. C **44**, 87 (2005).

[5] M. Burkardt, Phys. Rev. D **72**, 094020 (2005).

[6] M. Burkardt, Int. J. Mod. Phys. A **18**, 173 (2003).

[7] M. Burkardt, Phys. Rev. D **62**, 071503 (2000); **66**, 119903 (E) (2002); J. P. Ralston and B. Pire, Phys. Rev. D **66**, 111501 (2002).

[8] X. Ji, Phys. Rev. Lett. **78**, 610 (1997).

[9] D. Chakrabarti, R. Manohar, and A. Mukherjee, Phys. Rev. D **79**, 034006 (2009).

[10] H. Dahiya and A. Mukherjee, Phys. Rev. D **77**, 045032 (2008).

[11] S. J. Brodsky, D. Chakrabarti, A. Harindranath, A. Mukherjee, and J. P. Vary, Phys. Lett. B **641**, 440 (2006); , Phys. Rev. D **75**, 014003 (2007).

[12] R. Manohar, A. Mukherjee, and D. Chakrabarti, Phys. Rev. D **83**, 014004 (2011).

[13] N. Kumar and H. Dahiya, Int. J. Mod. Phys. A **30**, 1550010 (2015).

[14] C. Mondal and D. Chakrabarti, Eur. Phys. J. C **75**, 261 (2015).

[15] C. Adolph et al. (COMPASS Collaboration), Phys. Lett. B **731**, 19 (2014).

[16] R. Enberg, B. Pire, and L. Szymanowski, Eur. Phys. J. C **47**, 87 (2006).

[17] D. Yu. Ivanov, B. Pire, L. Szymanowski, and O. V. Teryaev, Phys. Lett. B **550**, 65 (2002); Phys. Part. Nucl. **35**, S67 (2004).

[18] S. V. Goloskokov and P. Kroll, Eur. Phys. J. C **74**, 2725 (2014).

[19] S. V. Goloskokov and P. Kroll, Eur. Phys. J. A **47**, 112 (2011).

[20] M. El Beiyad, B. Pire, M. Segond, L. Szymanowski, and S. Wallon, Phys. Lett. B **688**, 154 (2010).

[21] N. Kumar and H. Dahiya, Phys. Rev. D **91**, 114031 (2015).

[22] M. Göckeler, Ph. Hägler, R. Horsley, Y. Nakamura, D. Pleiter, P. E. L. Rakow, A. Schäfer, G. Schierholz, H. Stüben, and J. M. Zanotti (QCDSF and UKQCD Collaborations), Phys. Rev. Lett. **98**, 222001 (2007); Phys. Lett. B **627**, 113 (2005).

[23] P. Hagler, Phys. Rep. **490**, 49 (2010).

[24] P. Hagler, Phys. Lett. B **594**, 164 (2004).

[25] J. D. Bratt et al. (LHPC Collaboration), Phys. Rev. D **82**, 094502 (2010).

[26] T. Gutsche, V. E. Lyubovitskij, I. Schmidt, and A. Vega, Phys. Rev. D **89**, 054033 (2014).

[27] S. J. Brodsky and G. F. de Teramond, Phys. Rev. D **77**, 056007 (2008).

[28] S. J. Brodsky and G. F. de Téramond, arXiv:1203.4025.

[29] A. Vega, I. Schmidt, T. Gutsche, and V. E. Lyubovitskij, Phys. Rev. D **83**, 036001 (2011); **85**, 096004 (2012).

[30] D. Chakrabarti and C. Mondal, Phys. Rev. D **88**, 073006 (2013).

[31] D. Chakrabarti and C. Mondal, Eur. Phys. J. C **73**, 2671 (2013).

[32] D. Chakrabarti, C. Mondal, and A. Mukherjee, Phys. Rev. D **91**, 114026 (2015).

[33] T. Gutsche, V. E. Lyubovitskij, I. Schmidt, and A. Vega, Phys. Rev. D **91**, 054028 (2015).

[34] G. Karl and J. E. Paton, Phys. Rev. D **30**, 238 (1984).

[35] T. Ledwig, A. Silva, and H. C. Kim, Phys. Rev. D **82**, 034022 (2010).

[36] T. Ledwig and H. C. Kim, Phys. Rev. D **85**, 034041 (2012).

[37] M. Diehl, T. Feldman, R. Jacob, and P. Kroll, Eur. Phys. J. C **39**, 1 (2005).

[38] B. Pasquini and S. Boffi, Phys. Lett. B **653**, 23 (2007).